JMEPEG (2007) 16:73–79
DOI: 10.1007/s11665-006-9011-1

1059-9495/$19.00

Grain Boundary Segregation Behavior in 2.25Cr-1Mo Steel During Reversible Temper Embrittlement

M.A. Islam

(Submitted March 20, 2006)

Low alloy steels serving for a long time at high temperature, e.g., around 500 °C, are very sensitive to temper embrittlement due to segregation of various trace elements at prior austenite grain boundaries and/or carbide/matrix interfaces. This type of segregation in combination with various environmental effects can adversely affect the fracture resistance and fatigue crack propagation rate with subsequent change in fracture morphology of low alloy steels. This article describes the segregation behavior of various elements in 2.25Cr-1Mo pressure vessel steel investigated by AES, FEG-STEM, SEM, and EDS analyses. As confirmed by AES and FEG-STEM, phosphorus is found to be the main embrittling element for isothermal embrittlement. Sulfur and Mo segregation is only evident after longer embrittlement times. In the step-cooling embrittlement, phosphorus is still found to be the main embrittling element, but heavy segregation of sulfur in some isolated intergranular facets was also observed. For P segregation, a Mo-C-P interaction is observed, while sulfur segregation is attributed to site competition between sulfur and carbon atoms.

Keywords AES, isothermal embrittlement, reversible embrittlement, segregation, step cooling

1. Introduction

In the case of 2.25Cr-1Mo steel for fast fracture, it has been found that the brittle fracture behavior can be changed from its typical transgranular cleavage fracture to intergranular decohesion, if the impurity element segregation level at prior austenite grain boundaries exceeds a certain critical value (Ref 1-3). As for brittle fast fracture, impurity element segregation due to classical temper embrittlement can also change the fracture mode in fatigue failure and enhance the crack growth rate (Ref 4, 5). As a result, impurity element segregation at microstructural sites plays an important role to control the fracture toughness and fatigue life of many components. The aim of this work is to investigate the segregation behavior of trace elements in 2.25Cr-1Mo steel under different heat treatment conditions and to correlate the concentration of impurity elements identified by AES investigation with the fracture morphology of the steel at low temperature.

2. Experimental

2.1 Materials and Heat Treatment

The material used in this investigation was a commercial grade of 2.25Cr-1Mo steel whose composition is given in Table 1.

M.A. Islam, Materials and Metallurgical Engineering Department, Bangladesh University of Engineering and Technology (BUET), Dhaka 1000, Bangladesh. Contact e-mail: aminulislam_7136@yahoo.com.

In this investigation, the following microstructures were considered:

1. Quenched and fully tempered martensitic microstructures: quenched microstructures (quenched from 1100 °C after 2 h of austenitization at this temperature) tempered at 650 °C for 2 h (QT condition).
2. Lightly embrittled (isothermal) QT martensitic microstructures: QT condition embrittled for 24 h at 520 °C (QTLE condition).
3. Medium embrittled (isothermal) QT martensitic microstructures: QT condition embrittled for 96 h at 520 °C (QTME condition).
4. Heavily embrittled (isothermal) QT martensitic microstructures: QT condition embrittled for 210 h at 520 °C (QTHE condition).
5. Heavily embrittled (step cooling) QT martensitic microstructures: QT condition embrittled for an overall period of 210 hours under step cooling conditions (QTSE condition) as shown in Fig. 1.

2.2 Metallography

A detailed microstructural characterization of specimens under different heat treatment conditions used in this investigation has been performed using standard technique.

2.3 Mechanical Testing

Fatigue precracks were grown at room temperature according to BS7448 (Ref 6) at a constant R ratio (where R is defined

Table 1 Chemical composition of the steel (wt%)

C	Si	S	P	Mn	Ni	Cr	Mo	V	Cu
0.15	0.22	0.023	0.013	0.51	0.11	2.27	0.91	0.01	0.16

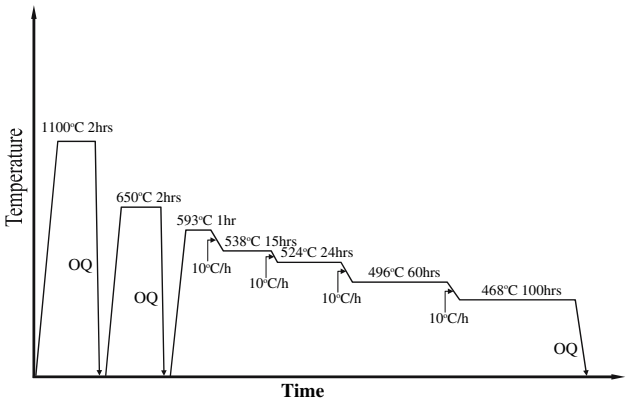

Fig. 1 Heat treatment cycle used for QTSE specimens

as P_{min}/P_{max}) of 0.1. The specimens were in their final heat-treated and machined condition. Using three point bending configuration, fracture toughness testing of the precracked specimens was carried out at −196 °C on a universal testing machine. During each test, the trace of load versus loading point displacement was plotted using an XY chart recorder. The values of fracture toughness, K_I were then measured by using the following equation:

$$K_I = \frac{FS}{BW^{1.5}} f(a_0/W),$$

where F, B, W, S, a_0, and $f(a_0/W)$ are, respectively, relevant load at brittle fracture, specimen thickness, width, span, effective crack length, and compliance function of the specimen.

2.4 Fractography

After fracture toughness tests, fracture surfaces were cut off the ends of specimens, using an abrasive cutting wheel for fractography. These fracture surfaces were then cleaned in an ultrasonic cleaner using acetone as the solvent, dried and mounted on aluminum stubs. Fractographic observations were then carried out in a scanning electron microscope (SEM) and the specimens were then photographed. Using these SEM micrographs, area fractions of intergranular fractures were measured either manually or automatically on a Quantimet-500 image analyser computer.

2.5 Energy Dispersive X-ray Microanalysis (EDS)

EDS microanalyses on clean transgranular cleavage facets and intergranular facets were carried out in the SEM with a LINK system energy dispersive X-ray spectrometer.

2.6 Auger Electron Spectroscopy (AES)

From each heat treatment condition, cylindrical specimens with a central notch were machined (Fig. 2) for Auger analysis to study the segregation behavior of various elements in the steel. The specimens were then cooled by liquid nitrogen in the Auger chamber under a high vacuum and broken. Immediately after fracture, grain boundary analysis was carried out as quickly as possible to avoid contamination in the vacuum chamber.

2.7 Transmission Electron Microscopy (TEM)

TEM samples of 3 mm diameter were cut and ground down to a thickness of approximately 0.07 mm. The discs were then jet polished at −30 °C in a solution of 5% perchloric acid and 95% ethanol with an electropolishing potential of 30 V and 1.5 A current. The transmission electron microscopy was performed using FEG-STEM with an operating voltage of 200 kV fitted with a LINK Oxford ISIS-300 system.

3. Results

3.1 Metallography

The optical micrographs of specimens under various heat treatment conditions exhibit mainly lath martensitic microstructures, which can be found elsewhere (Ref 2, 3).

3.2 Fracture Toughness (K_I) Values

The average K_I values for each condition are presented in Table 2. From this table, it is clear that temper embrittlement treatment decreased the average K_I values of QT samples. Having the similar level of exposure time, step-cooling embrittlement (QTSE condition) is found to be more severe compared to the isothermal embrittlement (QTHE condition) (Table 2).

3.3 Fractography

The fracture surfaces corresponding to the final fast fracture regions of all specimens, for each heat treatment condition, were examined closely in the SEM. The fracture surfaces associated with the catastrophic fractures observed for QT condition were almost 100% transgranular cleavage. Reversible

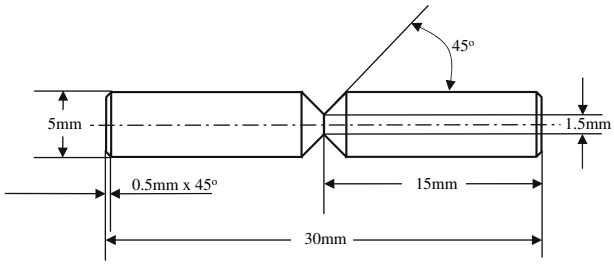

Fig. 2 AES specimen geometry

Table 2 Average fracture toughness values and % intergranular fractures of the steel under different heat treatment conditions and tested at −196 °C

	Fracture toughness measurements			
	K_{IC}, MPa√m		%I.G. fracture	
HT code	Average	SD	Average	SD
QT	45.5	±3.4	0	–
QTLE	42.1	±5.4	19	±12
QTME	36.1	±3.3	39	±11.2
QTHE	32.1	±2.6	65	±5.2
QTSE	30.8	±2.5	70	±5.1

temper embrittlement was found to change the fracture mode of the initial QT condition from transgranular cleavage to a mixed mode (transgranular cleavage and intergranular decohesion) of fracture (Ref 1-3). The area fraction of intergranular fracture was found to increase with embrittlement time (Table 2). From this table, it is also clear that step-cooling embrittlement (QTSE condition) produced a somewhat higher proportion of intergranular facets compared to isothermal embrittlement (QTHE condition) for the same extent of exposure.

3.4 Auger Electron Spectroscopy (AES)

Specimens in QT condition exhibited transgranular cleavage fracture surfaces at low temperatures, whereas mixed fracture modes (transgranular/intergranular) were observed for embrittled specimens (QTLE, QTME, QTHE, and QTSE conditions). The transgranular cleavage facets for QT specimen and intergranular facets for specimens of all embrittled conditions were analyzed using AES. The elements analyzed are Mo, Cr, P, S, C, O, and Fe.

3.4.1 Molybdenum. No molybdenum peak was observed on transgranular cleavage facets (Fig. 3). Auger spectra from intergranular facets of QTLE specimen showed a small Mo peak, Fig. 4 and it was found to increase with embrittlement time, Fig. 5 (QTME condition) and Fig. 6 (QTHE condition). The specimens of QTHE and QTSE conditions exhibited almost the same peak heights for Mo (Fig. 6 and 7).

3.4.2 Chromium. No significant segregation of this element above the bulk level (observed on the transgranular cleavage facet for QT condition) was detected for any embrittlement condition (Fig. 3-7).

3.4.3 Phosphorus. On the transgranular cleavage facet (QT condition) no phosphorus peak was observed, but from intergranular facets for all heat embrittlement conditions, peaks of this element were identified (Fig. 3-7) and the peak heights were found to increase steadily with the embrittlement time. Initially (24 h, QTLE condition) rapid segregation was observed and then the rate of segregation decreased (96 h, QTME condition and 210 h, QTHE condition and also for QTSE condition) (Table 3). For the same exposure time, a specimen subjected to a step-cooling embrittlement (QTSE

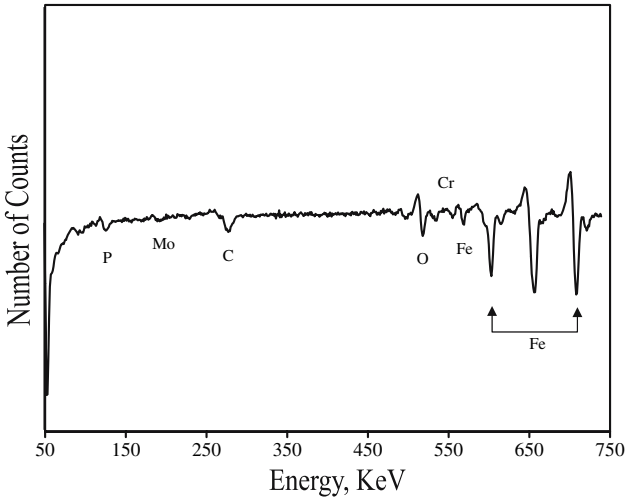

Fig. 4 Typical AES differential spectra taken from intergranular facet of QTLE specimen

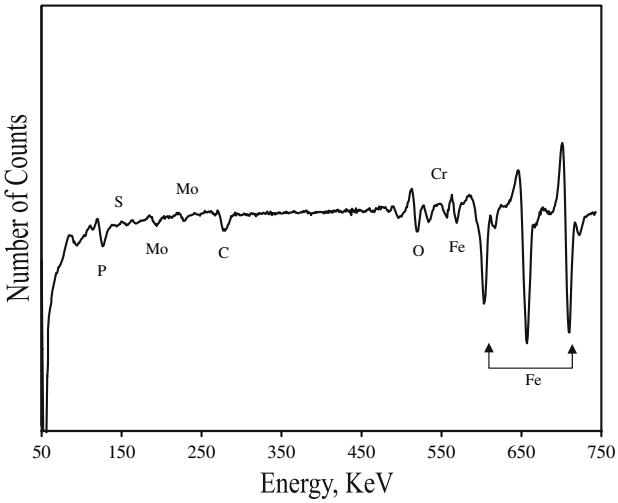

Fig. 5 Typical AES differential spectra taken from intergranular facet of QTME specimen

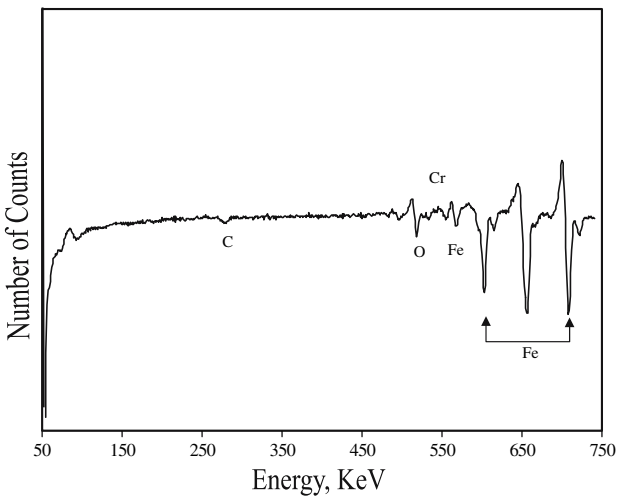

Fig. 3 AES differential spectra taken from a transgranular cleavage facet of QT specimen

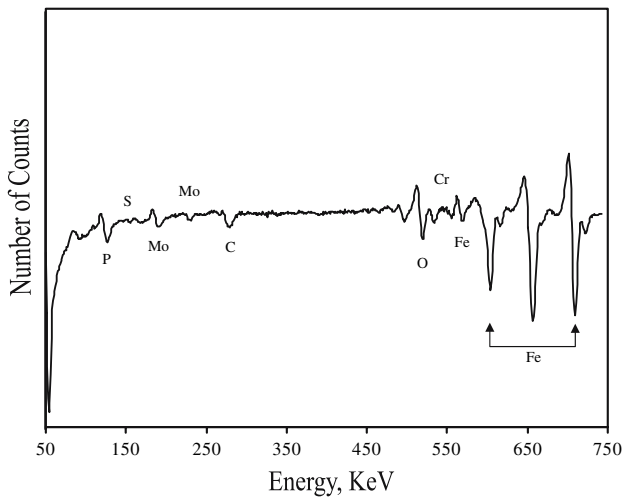

Fig. 6 AES differential spectra taken from intergranular facet of QTHE specimen

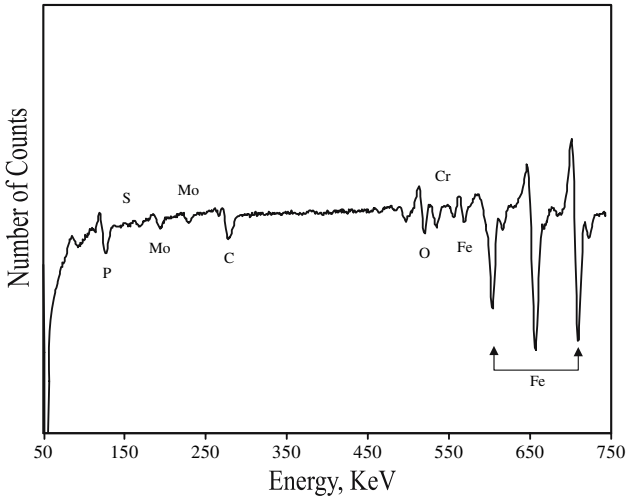

Fig. 7 AES differential spectra taken from intergranular facet of QTSE specimen

condition) showed a slight increase in P peak height compared with that for an isothermal embrittlement causing the same exposure time (QTHE condition) (Fig. 6 and 7).

3.4.4 Sulfur. As for phosphorus, sulfur was not found on transgranular cleavage facets for QT specimens. For embrittled specimens, some marked differences between the segregation of S and P were observed:

(1) For short embrittlement periods (QTLE condition, Fig. 4) no noticeable sulfur segregation was observed. Peaks from this element are only prominent for longer embrittlement times (Fig. 5-7).
(2) The sulfur peaks for isothermally embrittled specimens are always smaller than the phosphorus peaks for the same intergranular facet.
(3) For specimens embrittled by step cooling, an interesting observation is that some intergranular facets exhibited large sulfur peaks and the phosphorus peak was almost absent (Fig. 8, 9, 10).
(4) A connection between sulfur and carbon segregation is observed. The sulfur peaks were found to increase as carbon peaks decreased (Fig. 6–8).

3.4.5 Carbon. This element was found on both transgranular cleavage and intergranular facets. The carbon peak on intergranular facets (embrittled condition) was found to be higher than that on transgranular cleavage facet (unembrittled condition). No marked variation in the carbon peaks was found with embrittlement time.

3.4.6 Oxygen. This element was observed on specimens for all heat treatment conditions. It is thought that oxygen peak from the fracture surface was due to adsorbed oxygen contamination in the vacuum chamber during analysis.

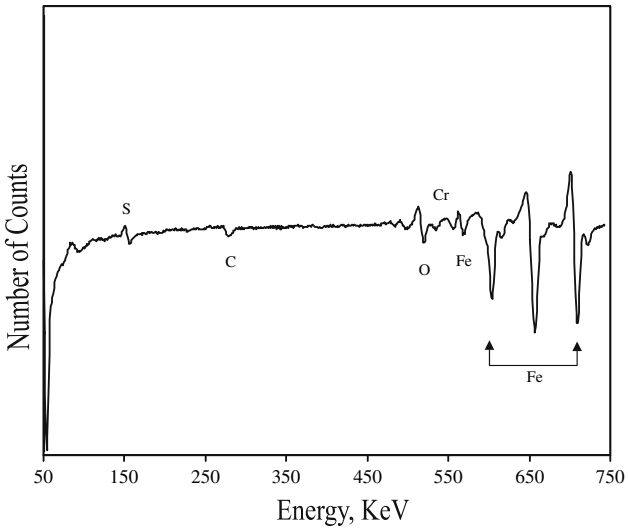

Fig. 8 Typical AES differential spectra taken from sulfur segregated intergranular facet of QTSE specimen. Note that this facet is almost P free

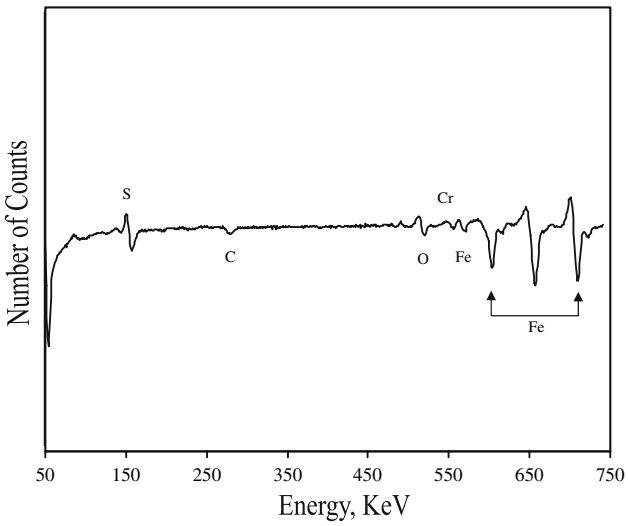

Fig. 9 Typical AES differential spectra taken from sulfur segregated intergranular facet of QTSE specimen

Table 3 The Auger %PHR of P(P_{120}/Fe_{703}), S(S_{152}/Fe_{703}), Mo(Mo_{186}/Fe_{703}), and C(C_{272}/Fe_{703}) for different embrittlement conditions

	P		S		Mo		C	
HT code	Average, %	SD	Average, %	SD	Average, %	SD	Average, %	SD
QTLE	11.4	±1.5	–	–	3.8	±0.6	14.5	1.8
QTME	15.6	±1.7	2.9	±0.5	5.8	±0.7	13.1	1.6
QTHE	18.8	±1.8	3.8	±0.7	7.9	±1.0	13.8	1.7
QTSE	19.2	±1.9	4.1	±0.7	7.8	±0.8	14.3	1.8

The Auger %PHR of P(P_{120}/Fe_{703}), S(S_{152}/Fe_{703}), Mo (Mo_{186}/Fe_{703}), and C(C_{272}/Fe_{703}) values are presented in Table 3.

3.5 Energy Dispersive X-Ray Microanalysis (EDS)

EDS analysis on transgranular cleavage and intergranular facets clearly identified Mo on the grain boundaries of QTHE specimen whereas it was absent on the transgranular cleavage facet of the same specimen (Fig. 11 and 12). From these figures, it is also clear that the Cr peaks from both the cleavage and intergranular facets are almost the same, which also support the AES results concerning the Cr segregation.

3.6 Transmission Electron Microscopy (TEM)

QT specimen exhibited the transgranular cleavage fracture, so AES analysis on grain boundary could not be carried out for specimens under this condition. The opportunity was taken for grain boundary analysis in the TEM. The TEM analysis clearly identified P and Mo at this grain boundary of QT specimen (Fig. 13).

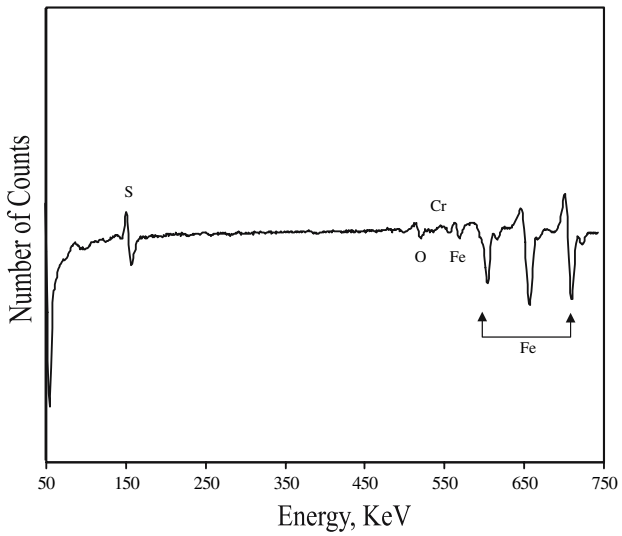

Fig. 10 Typical AES differential spectra taken from sulfur segregated intergranular facet of QTSE specimen. Note that C peak is almost absent and the S peak is very large

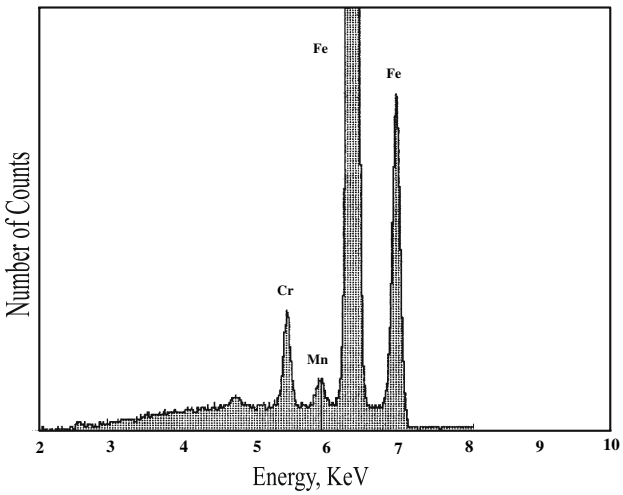

Fig. 11 EDS analysis on a transgranular cleavage facet of QTHE specimen

4. Discussion

4.1 Fracture Toughness (K_I Values)

Table 2 illustrates the average fracture toughness values of specimens under different heat treatment conditions at −196 °C. As can be seen from Table 2, reversible temper embrittlement was found to reduce the average fracture toughness value of QT specimens and the decrease in fracture toughness values is a function of embrittlement time. Another observation is that the QTSE condition showed slightly lower average fracture toughness value than the QTHE condition, although specimens under these two heat treatment conditions experienced approximately similar level of exposure time.

It is now generally accepted that the impurity element segregation to prior austenite grain boundaries changes the fracture mode of low alloy ferritic steels from a typical transgranular cleavage fracture to intergranular decohesion, resulting a decrease in the fracture toughness value. When the fracture mode is of a mixed type, the proportion of intergranular fracture can also affect the fracture toughness value. In this context, attention has been drawn to the variation of fracture toughness with the area fraction of intergranular facets in 2.25Cr-1Mo pressure vessel steel under conditions of as-quenched and reversible temper embrittlement (Ref 2). Naudin et al. (Ref 7) demonstrated that with increase in the degree of grain boundary segregation, the percentage of intergranular fracture increases and the intergranular fracture stress decreases. As the increased level of segregation caused higher proportion of intergranular fracture from QTLE condition through QTME condition to QTHE condition, the fracture toughness values also decreased progressively.

From Table 2, it is also clear that QTSE condition resulted relatively lower fracture toughness values compared to that of QTHE condition. The reason is that specimens in this group produced higher proportion of intergranular fracture. As the proportion of intergranular fracture controls the fracture toughness value, QTSE specimens resulted lower average fracture toughness value.

4.2 Fractography

QT specimens failed by 100% transgranular cleavage fracture, whereas a mixture of intergranular facets and transgranular cleavage facets was observed on the fracture faces of QTLE, QTME, QTHE, and QTSE conditions (Table 2). It has also been observed that the area fractions of intergranular facets increased and the fracture toughness values decreased with embrittlement time (Table 2). In general, transgranular cleavage is typical for the brittle fracture mode of unembrittled ferritic steels. During temper embrittlement, trace impurity elements belonging to groups IV-VI in the Periodic Table (e.g., S, P, Sb, As, Sn, etc.) segregate to microstructural sites such as prior austenite grain boundaries and carbide/matrix interfaces. Such segregation decreases the interfacial cohesive strength and changes the brittle fracture mode from a typical transgranular cleavage fracture to intergranular decohesion. Auger analysis of these grain boundary facets, in all heat treatment conditions,

showed that the intergranular decohesion observed in the present study is mainly due to phosphorus segregation.

4.3 Observation of Segregation Behavior

AES analysis detected Mo on intergranular facets of all embrittled specimens and in general, Mo peaks were found to increase with the embrittlement time. The chemical state of this element is, however, not certain. The saturation level of dissolved Mo in α-iron is ~0.7% (Ref 8). When the Mo content is beyond this level, Mo-rich carbide starts to precipitate, whereas in the present steel the Mo content is about 0.9%. It has also been observed that a gradual replacement of M_3C carbide by M_2C carbide takes place during the embrittlement (Ref 9, 10). In this study, EDS microanalysis confirmed that the coarse carbides were Mo-rich (Ref 11). Mo atoms on the intergranular facets could, therefore, be present in the form of Mo-rich fine carbides. However, the increase in Mo peak height with P peak height supports the possibility of Mo-P co-segregation. Figure; 11 and 12, respectively, represent the EDS spectra from a clean transgranular cleavage facet and a clean intergranular facet of QTHE specimen. The presence of a Mo peak in Fig. 12 also indicates the possibility of Mo segregation. As a result, Mo atoms on the intergranular facet detected by AES (see also TEM trace for Mo in Fig. 13) may be present in the form of grain boundary fine carbides and/or as segregation atoms (Mo-P clusters).

For any of the embrittlement treatments no noticeable segregation of Cr above the bulk level was observed using AES analysis (Fig. 3-10). EDS analysis also supports this AES observation concerning the Cr segregation (Fig. 11 and 12). With increasing embrittlement time, P peak heights increased, but Cr peaks remained almost unchanged. During tempering and embrittlement, carbide phase changes in 2.25Cr-1Mo steel are now well documented, but no marked change in the Auger peak of Cr was observed. In M_3C carbides the concentration of Cr is ~12 at.%, whereas in M_2C carbide, it can be up to ~14 at.% (Ref 10). This indicates that apparently there should be a little change in Cr concentration in the matrix as a result of the carbide phase changes (from M_3C to M_2C). Carbon was detected on both transgranular cleavage (unembrittled condition) and intergranular facets (embrittled conditions). For the intergranular facets, the carbon peaks were higher than that for the transgranular cleavage facets, however, no further increase was observed with embrittlement time.

Phosphorus was found to segregate in specimens under all embrittlement conditions. With increase in embrittlement time the P concentration on grain boundary facets was found to increase (Table 3), which is in agreement with the observations of other researchers (Ref 7, 8). As the degree of segregation increases, the intergranular cohesive strength of the steel also decreases, which causes a significant decrease in the fracture toughness values.

From Table 3, the average Auger %PHR (P_{120}/Fe_{703}) after 24 h aging (QTLE condition) is 11.4%, for 96 h (QTME condition) 15.6% and for 210 h (QTHE condition) 18.8%. For aging periods of 24, 96, and 210 h, the aging time: %PHR of P are, respectively, 1:0.48, 1:0.16, and 1:0.09. This observation indicates that the P segregation has slowed down significantly with increasing aging time, which is consistent with the segregation behavior of impurity elements during isothermal embrittlement (Ref 7, 12).

Sulfur was not found to show strong segregation behavior for isothermal embrittlement. Although Auger analysis detected S atoms along with P atoms on isothermally embrittled specimens, S segregation was only prominent for longer exposure periods. The reason may be due to the interaction of S with Mn. Mn has a very strong affinity to S and it forms MnS and reduces the free sulfur in the matrix: as a result, sulfur segregation becomes negligible (Ref 13). For QTSE specimens, an interesting observation is that some intergranular facets showed a strong S peak (Fig. 8-10). Briant and Banerji (Ref 14) found this type of segregation behavior for Ni-Cr steel under

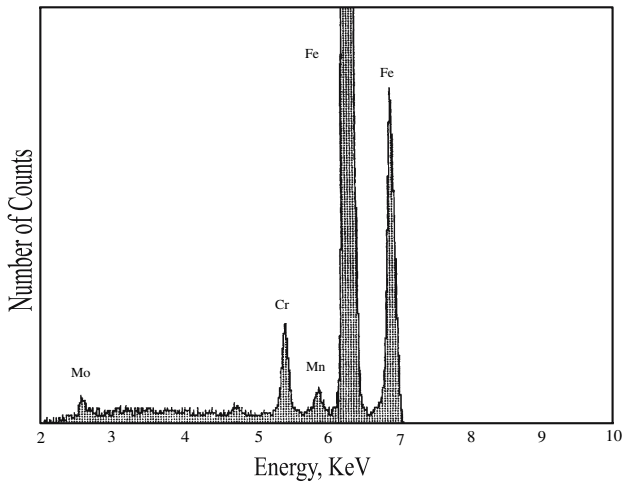

Fig. 12 EDS analysis on a clean intergranular facet of QTHE specimen

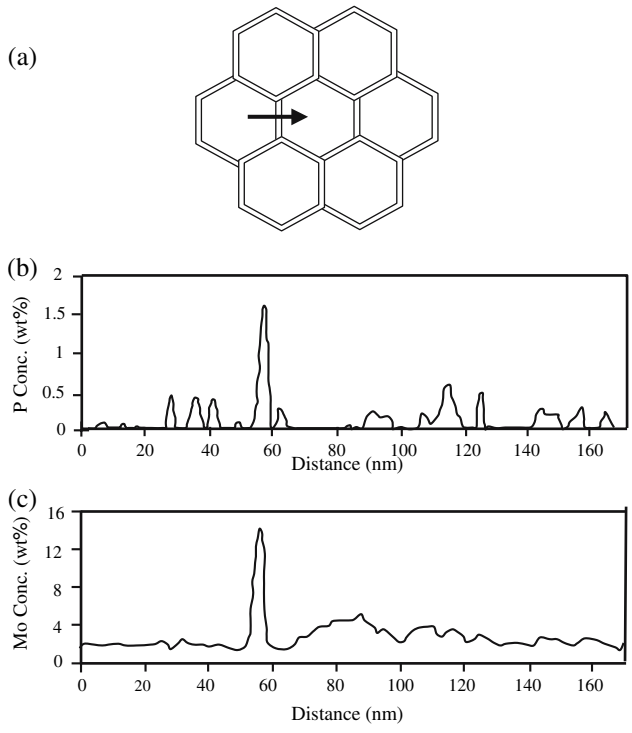

Fig. 13 (a) Direction of TEM analysis across the grain boundary (marked by arrow) on QT specimen, (b) variation in P concentration, and (c) variation in Mo concentration across the boundary

one-step-temper-embrittlement condition. For this heat treatment condition, they found both P and S segregation, but Auger analysis on some individual grains showed only S, which is thought due to the non-homogeneity in chemical composition in the steel.

From the Auger spectra presented in Fig. 8-10, the S peaks are very clear, whereas P and Mo peaks are almost absent. This observation suggests that S segregation is not related to Mo segregation. Another interesting observation is the dependence of S peaks on carbon peaks. As carbon peaks decrease, S peaks increase. This observation suggests that there is a connection between the relative segregation behavior of S and C. Many investigators (Ref 15, 16) drew attention to the site competition between S and C. Due to compositional inhomogeneties, it may happen that some grains have higher S content but lower carbon content. In the low carbon content regions, the possibility of Mo-based alloy carbide formation is low, so there is no or very little precipitation of Mo-rich carbides on these grain boundaries. As a result, Mo will arguably remain as Mo-P clusters and the P segregation will be inhibited, so there may be a synergistic relationship between S segregation and carbon content.

5. Conclusions

1. Phosphorus has been found to be the main embrittling element for all embrittlement treatments, however, heavy segregation of sulfur in some isolated intergranular facets has also been observed.
2. For phosphorus segregation, a Mo-C-P interaction is observed, while for sulfur segregation is attributed due a synergistic site competition between sulfur and carbon atoms.
3. Chromium has not been found to segregate and/or to influence the segregation behavior in the steel under the present heat treatment conditions.
4. With an increase in embrittlement time, the %PHR (P_{120}/Fe_{703}) increased, which is thought to be the basic cause for the increase in the percentage of intergranular facets on the fracture surfaces and the decrease in the fracture toughness values at low temperatures.

Acknowledgments

The author is highly grateful to ORS Authority of U.K. and also Professor J.F. Knott and Professor P. Bowen of School of Metallurgy and Materials, University of Birmingham, U.K. to provide financial help during this research work. He also acknowledges Chris Hardy for her co-operation during AES analysis.

References

1. M.A. Islam, J.F. Knott, and P. Bowen, Critical Level of Intergranular Fracture to Affect the Toughness of Embrittled 2.25Cr-1Mo Steels, *J. Mater. Eng. Perform.*, 2004, **13**(5), p 600–606
2. M.A. Islam, "Intergranular Fracture in 2.25Cr-1Mo Pressure Vessel Steel at Low Temperatures," Ph.D. Thesis, The University of Birmingham, U.K., 2001
3. M.A. Islam, M. Novovic, P. Bowen, and J.F. Knott, Effect of Phosphorus Segregation on Fracture Properties of 2.25Cr-1Mo Pressure Vessel Steel, *J. Mater. Eng. Perform.*, 2003, **12**(3), p 244–248
4. K. Nishioka and J.F. Knott, *Effects of Environment on the Occurrence of Intergranular Facets During Fatigue Crack Propagation in 9Cr-1Mo Steel*. Mech. Engr. Publications, London, 1990, 241–254
5. M.A. Islam, P. Bowen, and J.F. Knott, Intergranular Fracture on Fatigue Fracture Surface of 2.25Cr-1Mo Steel at Room Temperature in Air, *J. Mater. Eng. Perform.*, 2005, **14**(1), p 28–36
6. BS 7448 "Fracture Mechanics Toughness Tests, Part 1, Method for Determination of KIC, Critical CTOD and Critical J Values of Metallic Materials," 1991, p 2677-2710
7. C. Naudin, J.M. Frund, and A. Pineau, Intergranular Fracture Stress and Phosphorus Grain Boundary Segregation of a Mn-Ni-Mo Steel, *Scripta Mater.*, 1999, **40**, p 1013–1019
8. J. Yu and C.J. McMahon Jr., Effect of Composition and Carbide Precipitation on Temper Embrittlement of 2.25Cr-1Mo Steel: Part 1. Effect of P and Sn, *Met. Trans.*, 1980, **11A**, p 277–289
9. R.C. Thomson and M.K. Miller, Carbide Precipitation in Martensite During the Early Stages of Tempering in Cr-and-Mo-Containing Low Alloy Steels, *Acta Mater.*, 1998, **46**(6), p 2203–2213
10. M. Wada, K. Hosoi, and O. Nishiwaka, FIM Observation of 2.25Cr-1Mo Steel, *Acta Metall.*, 1982, **30**, p 1005–1011
11. M.A. Islam, J.F. Knott, and P. Bowen, Kinetics of Phosphorus Segregation and its Effect on Low Temperature Fracture Behaviour in 2.25Cr-1Mo Pressure Vessel Steel, *J. Mater. Sci. Technol.*, 2005, **21**(1), p 76–84
12. T. Wada and W.C. Hagel, Effect of Trace Elements, Molybdenum and Intercritical HT on Temper Embrittlement of 2.25Cr-1Mo Steel, *Met. Trans. A*, 1976, **7A**, p 1419–1426
13. J. Yu and C.J. McMahon Jr., Effect of Composition and Carbide Precipitation on Temper Embrittlement of 2.25Cr-1Mo Steel: Part 2. Effect of Mn and Si, *Met. Trans.*, 1980, **11A**, p 291–300
14. C.L. Briant and S.K. Banerji, Phosphorus Induced 350 °C Embrittlement in an Ultra High Strength Steel, *Met. Trans. A*, 1979, **10**, p 123–131
15. K.S. Shin and T. Tsao, Effect of Carbon on Grain Boundary Segregation of Sulfur in Iron, *Scripta Metall.*, 1988, **22**, p 585–588
16. S. Suzuki, M. Obata, K. Abiko, and H. Kimura, Effect of Carbon on the Grain Boundary Segregation of P in Alpha-iron, *Scripta Metall.*, 1983, **17**, p 1325–1328